

# 1    **Direct inhibitors of InhA with efficacy similar** 2    **or superior to isoniazid in novel drug** 3    **regimens for tuberculosis**

4    Lourdes Encinas, <sup>a</sup> Si-Yang Li, <sup>b</sup> Joaquin Rullas-Trincado, <sup>a</sup> Rokeya Tasneen, <sup>b</sup>  
5    Sandeep Tyagi, <sup>b</sup> Heena Soni, <sup>b</sup> Adolfo Garcia-Perez, <sup>c</sup> Jin Lee, <sup>b</sup> Rubén González del  
6    Rio, <sup>a</sup> Jaime De Mercado, <sup>c</sup> Verónica Sousa, <sup>b</sup> Izidor Sosič, <sup>d</sup> Stanislav Gobec <sup>d</sup> Alfonso  
7    Mendoza-Losana, <sup>a§</sup> Paul J. Converse, <sup>b</sup> Khisi Mdluli, <sup>e¶</sup> Nader Fotouhi, <sup>e</sup> David Barros-  
8    Aguirre, <sup>a</sup> Eric L. Nuermberger, <sup>b</sup>

9

10    <sup>a</sup> Global Health Medicines R&D, GSK, c/ Severo Ochoa, 2, 28760, Tres Cantos, Madrid,  
11    Spain

12    <sup>b</sup> Center for Tuberculosis Research, Division of Infectious Diseases, Johns Hopkins  
13    University, Baltimore, MD, USA

14    <sup>c</sup> Discovery DMPK, GSK, c/ Severo Ochoa, 2, 28760, Tres Cantos, Madrid, Spain

15    <sup>d</sup> Faculty of Pharmacy, University of Ljubljana, Aškerčeva 7, 1000, Ljubljana, Slovenia.

16    <sup>e</sup> TB Alliance: Global Alliance for Tuberculosis Drug Development, New York, New York,  
17    USA

18    Running Head: Direct InhA inhibitors improve TB regimens in mice

19    #Address correspondence to Eric L. Nuermberger, [enuermb@jhmi.edu](mailto:enuermb@jhmi.edu); Lourdes  
20    Encinas, [lourdes.p.encinas-prieto@gsk.com](mailto:lourdes.p.encinas-prieto@gsk.com)

21    <sup>¶</sup> Present address: Khisimuzi Mdluli, Bill & Melinda Gates Medical Research Institute,  
22    Cambridge, Massachusetts, USA.

23    <sup>§</sup> Present address: Alfonso Mendoza-Losana, Department of Bioengineering and  
24    Aerospace Engineering, Carlos III University of Madrid, 28040 Madrid, Spain.

25

26

27 **ABSTRACT**

28 **Isoniazid is an important first-line medicine to treat tuberculosis (TB). Isoniazid**  
29 **resistance increases the risk of poor treatment outcomes and development of**  
30 **multidrug resistance, and is driven primarily by mutations involving *katG*,**  
31 **encoding the pro-drug activating enzyme, rather than its validated target, InhA.**  
32 **The chemical tractability of InhA has fostered efforts to discover direct inhibitors**  
33 **of InhA (DIIs). During the past five years, successful target engagement and *in***  
34 ***vivo* efficacy have been demonstrated by diverse DIIs. In this study, we bridge the**  
35 **gap in understanding the potential contribution of DIIs to novel combination**  
36 **regimens and demonstrate a clear distinction of DIIs, like GSK693 and the newly**  
37 **described GSK138, from isoniazid, based on activity against clinical isolates and**  
38 **contribution to novel drug regimens. The results presented increase the**  
39 **understanding of DII mechanism of action and provide further impetus to**  
40 **continue exploiting InhA as a promising target for TB drug development.**

41 **INTRODUCTION**

42 Tuberculosis (TB) is a communicable disease caused by *Mycobacterium tuberculosis*  
43 (*M.tb*). Globally, an estimated 10.6 million people developed TB in 2022, up from best  
44 estimates of 10.3 million in 2021 and 10.0 million in 2020. Until the coronavirus (COVID-  
45 19) pandemic, TB was the leading cause of death from a single infectious agent,  
46 ranking above HIV/AIDS. The COVID-19 pandemic has had a negative impact on  
47 access to TB diagnosis and treatment as well as the burden of TB disease. The  
48 estimated number of deaths from TB increased between 2019 and 2021, reversing  
49 years of decline. An estimated total of 1.3 million people died from TB in 2022 (including

50 167,000 people with HIV). The net reduction in the global number of deaths caused by  
51 TB from 2015 to 2022 was 19%, far from the WHO End TB Strategy milestone of a 75%  
52 reduction by 2025 (1, 2). With timely diagnosis and treatment with first-line drugs, most  
53 people who develop TB are cured and onward transmission of infection is curtailed. The  
54 currently recommended treatment for drug-susceptible pulmonary TB is a 6-month  
55 regimen consisting of an *intensive phase* of 2 months with a 4-drug regimen of  
56 isoniazid, rifampicin, pyrazinamide, and ethambutol, followed by a *continuation phase* of  
57 four months with isoniazid and rifampicin.

58 Isoniazid was discovered in 1952 and has been widely used to treat TB ever since (3). It  
59 is a prodrug that requires activation by the mycobacterial catalase-peroxidase enzyme  
60 KatG to form the reactive isonicotinyl acyl radical (4), which then forms a covalent  
61 adduct with the cofactor nicotinamide adenine dinucleotide (isoniazid-NAD adduct) (5).  
62 This adduct is the inhibitor of the mycobacterial fatty acid synthase II (FAS-II)  
63 component enoyl-acyl carrier protein reductase (InhA), which is required for the  
64 synthesis of mycolic acids, a central component of the mycobacterial cell wall (6, 7).

65 Isoniazid is an important first-line TB drug. Baseline isoniazid resistance increases the  
66 risk of poor treatment outcomes (e.g. treatment failure or relapse) and acquisition of  
67 multidrug-resistant (MDR) TB. Based on evidence reviews indicating reduced efficacy of  
68 the standard first-line drugs for the treatment of isoniazid-resistant TB (Hr-TB) (8-13),  
69 the World Health Organization (WHO) issued a Supplement to its guidelines for the  
70 treatment of drug-resistant TB in 2018, providing new recommendations for the  
71 management of Hr-TB (14). Resistance to isoniazid is primarily caused by mutations in  
72 the activating enzyme KatG or in the upstream promoter region of InhA or more rarely in

73 the InhA enzyme itself. Combinations of these mutations may also occur. By and large,  
74 the most common mutations in Hr-TB strains are found in *katG* and confer “high-level”  
75 resistance, even in the absence of an *inhA* mutation. In this situation, the inclusion of  
76 isoniazid in the regimen, even at high doses, is unlikely to increase its effectiveness  
77 (although this question is currently under investigation: *ClinicalTrials.gov Identifier:*  
78 *NCT01936831*). On the other hand, mutations in the *inhA* promoter or in the *inhA* gene  
79 are generally associated with lower-level resistance than *katG* mutations, and higher  
80 doses of isoniazid (10-15 mg/kg/day) may result in bactericidal activity against such  
81 *inhA* mutants similar to that observed with standard isoniazid doses (4-6 mg/kg/day)  
82 against fully susceptible strains (4, 15-17).

83 The opportunity to overcome the high rate of clinical resistance to isoniazid due to *katG*  
84 mutations, together with the biological relevance of InhA (target validated clinically by  
85 isoniazid and ethionamide) and its chemical tractability, (18) has fostered efforts to  
86 discover direct inhibitors of InhA (DIIs). During the last five years, three structurally  
87 different molecules have demonstrated *in vivo* efficacy in murine TB  
88 models upon oral administration: **NITD-916** (19), **GSK2505693A (GSK693)** (20) and  
89 **AN12855** (21).

## 90 **RESULTS**

91 To our knowledge, **GSK693** was the first DII compound to demonstrate *in vivo* efficacy  
92 comparable to that of isoniazid (20). More recently, Xia and coauthors reported the  
93 discovery of a direct, cofactor-independent inhibitor of InhA, AN12855, which showed  
94 good efficacy in acute and chronic murine TB models that was also comparable to

95 isoniazid (20). The high preliminary human dose prediction of **GSK693** hampered its  
96 further development as a lead compound. Within the same thiadiazole-based series,  
97 **GSK3081138A (GSK138)**, a structurally very similar and slightly more lipophilic  
98 compound, was selected as a back-up compound based on its balanced profile of  
99 physicochemical properties, *in vitro* potency, *in vivo* pharmacokinetics (PK), and safety  
100 (Table 1).

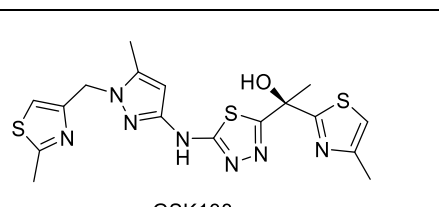
101 **GSK138** is a medium molecular weight compound with a chrom logD at pH 7.4 of 3.38.  
102 The measured solubility in Fasted State Simulated Intestinal Fluid (FaSSIF) was high  
103 (Table 1). The permeability of **GSK138** predicted from Madin-Darby Canine Kidney  
104 (MDCK) cells was also high (Table 1). The efflux ratio determined by assays with and  
105 without incubation with a potent P-glycoprotein (P-gp) inhibitor indicated that it is a P-gp  
106 substrate.

107 **GSK138** inhibited recombinant InhA with an IC<sub>50</sub> of 0.04  $\mu$ M. The MIC was 1  $\mu$ M against  
108 *M. tuberculosis* H37Rv and **GSK138** retained its activity against intracellular bacteria  
109 growing inside THP-1-derived macrophages *in vitro* (MIC 0.9  $\mu$ M). Additionally, it  
110 showed no effect up to the highest concentration tested (200  $\mu$ M) in the Cell Health  
111 assay (measuring membrane, nuclear, and mitochondrial damage). The preliminary  
112 toxicological profile showed an overall clean *in vitro* safety profile.

113 To assess the susceptibility of **GSK138** to P450-mediated phase I metabolism,  
114 metabolic stability was determined during incubation in CD1 mouse, Sprague Dawley  
115 rat, beagle dog, and human liver microsomes. **GSK138** exhibited moderate *in vitro*  
116 clearance in liver microsomes from the pre-clinical species, and low *in vitro* clearance in  
117 humans.

118 To determine the pharmacokinetic parameters, **GSK138** was administered  
119 intravenously (formulation: 5%DMSO/20%Encapsin in saline solution) as a single bolus  
120 dose in C57BL/6 mice at a target dose of 1 mg/Kg. All pharmacokinetic parameters  
121 were determined in whole blood (Table 1). A moderate clearance and a moderate  
122 volume of distribution were observed.

123  
124 TABLE 1. Structure and properties of the optimized lead **GSK138**. The lead was assessed for  
125 activity against *M. tuberculosis* H37Rv both intracellularly and extracellularly. The  
126 physicochemical and ADMET properties were determined as well.

 GSK138		
<b>Physicochemical properties</b>	MW	433
	clogP/Chrom logD	1.2/3.39
	Permeability Papp (MDCK-MDR1)	374 nm/s
	Solubility FaSSIF (pH 6.5)	140-320 $\mu$ M
<b>Activity profile</b>	InhA IC <sub>50</sub> <sup>*</sup>	0.04 $\mu$ M $\pm$ 0.01
	<i>Mtb</i> MIC	1 $\mu$ M
	<i>Mtb</i> intracell MIC <sup>*</sup>	0.9 $\mu$ M $\pm$ 0.1
<b>Cytotoxicity profile</b>	HepG2 Cytotoxicity Tox <sub>50</sub>	>100 $\mu$ M
	Cell Health (nuclear size, mitochondrial membrane potential and plasma membrane permeability)	>199.5 $\mu$ M
<b>Genetic toxicity assessment</b>	Ames test	Negative
<b>Cardiovascular profile</b>	hERG Qpatch IC <sub>50</sub>	>30 $\mu$ M
<b>Microsomal stability assessment</b>	<i>In vitro</i> Cli mouse/rat/dog/human	4.4 /3.5/1.7/0.3 mL/min/g tissue
<b><i>In vivo</i> pharmacokinetic profile</b>	<i>In vivo</i> Cl mouse (1 mg/Kg iv <sup>*</sup>	77.6 $\pm$ 16.8 mL/min/Kg
	<i>In vivo</i> Vss mouse (1 mg/Kg iv) <sup>*</sup>	2.6 $\pm$ 0.3 L/Kg

127 \*mean  $\pm$  Standard Deviation.  
128

129 The minimum concentrations of **GSK693** and **GSK138** that inhibit 90% of isolates  
130 tested ( $\text{MIC}_{90}$ ) were determined against a set of drug-susceptible, multidrug-resistant  
131 (MDR) and extensively drug-resistant (XDR) *M.tb* clinical isolates. Both **GSK693** and  
132 **GSK138** retained activity against these clinical isolates (**GSK693**  $\text{MIC}_{90} = 1.87 \mu\text{M}$ ;  
133 **GSK138**  $\text{MIC}_{90} = 3.75 \mu\text{M}$ ), similar to the MICs against strain H37Rv in the same assay  
134 (Table 2). As expected for DIs, the thiadiazole compounds have KatG-independent  
135 activity. No change in MIC was observed against isonazid-resistant clinical isolates  
136 carrying mutations in *katG* S315T. Clinical isolates carrying an *inhA* C-15T mutation  
137 have increased InhA production which confers low-level resistance to isoniazid. Among  
138 eight clinical isolates with the *inhA* C-15T mutation, three showed low-level resistance to  
139 the thiadiazoles (i.e., MICs for both DIs  $\geq 4$  times the MIC against strain H37Rv).  
140 Thiadiazoles remained equally effective among the rest of the sensitive, MDR and XDR  
141 *M.tb* clinical isolates tested.

142  
143 TABLE 2. Activity of **GSK693** and **GSK138** against resistant *M.tb* clinical isolates obtained from  
144 Vall d'Hebron Hospital, Barcelona. Resistance pattern: **H** = isoniazid (*katG* S315T mutation:**G**),  
145 **inhA** promoter C-15T mutation:**P**), R = rifampicin, Z = pyrazinamide, M = moxifloxacin, T =  
146 ethionamide, S = streptomycin, E = ethambutol, K = kanamycin, A = amikacin, Cm =  
147 capreomycin, O = ofloxacin, Cp = ciprofloxacin, and Pas = para-aminosalicylic acid

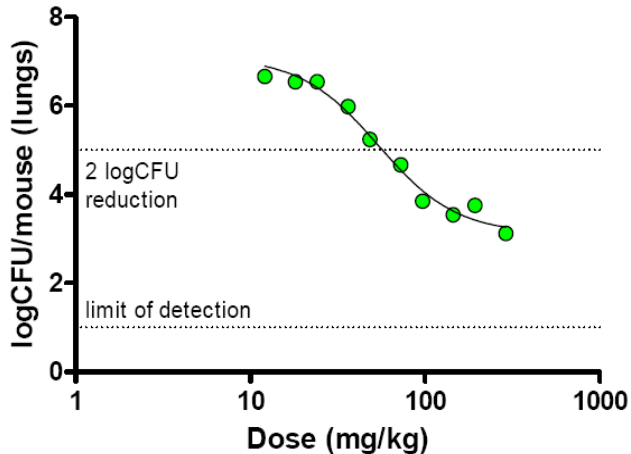
148

Strain #	Strain ID	Resistance	693 MIC ( $\mu\text{M}$ )	138 MIC ( $\mu\text{M}$ )
1	13243	MOCp	<0.23	<0.23
2	12569	OCp	<0.23	<0.23
3	9685A	<b>H(G)RESZCpT</b>	<0.23	<0.23
4	7788	RZCmK	<0.23	0.23
5	14388	<b>H(G)RESZCmAT</b>	<0.23	0.47
6	13026	<b>H(G)RESCmKcpO</b>	<0.23	0.47
7	13214	<b>H(P)SPas</b>	<0.23	0.47
8	12733	<b>H(G)EZOTPAs</b>	<0.23	0.47
9	7957	KCp	<0.23	0.47

10	10841	H(G)RESZMO	<0.23	0.47	
11	10071	H(G)RESZKCp	<0.23	0.47	
12	11881	H(G)RESZCmKCp	<0.23	0.47	
13	8059	Cp	<0.23	0.47	
14	14294	ZMO	0.23	0.23	
15	11341	H(G)REOPas	0.23	0.47	
16	13830	H(G)RESZCmKMO	0.47	0.47	
17	14379	H(G)RESZMO	0.47	0.47	
18	14883	H(G)RESZCp	0.47	0.94	
19	13222	SCmMCpO	0.47	0.94	
20	10492	RSCp	0.47	0.94	
21	11586	H(G)RESKCP	0.94	1.875	
22	11347	H(P)RECmKO	0.94	1.875	
23	10027	H(G)RESZCmKCp	0.94	1.875	
24	7786	H(P)RESCmKCp	1.875	1.875	
25	10190	H(P)REZCp	1.875	1.875	
26	7543	H(P)RESZCmKCp	1.875	1.875	
27	11366	H(GP)RESCmKO	1.875	3.75	
28	11348	H(P)RESOTPAs	3.75	7.5	
29	13229	H(P)RZMCpOT	7.5	>15	
30	H37Rv	Susceptible (control)	<0.23	0.94	
31	14639	Susceptible (control)	0.47	0.47	

149

150 Based on **GSK138**'s overall profile, the therapeutic efficacy of **GSK138** against *M.tb* in  
151 an acute murine model of intratracheal infection was determined (see FIG 1).



152

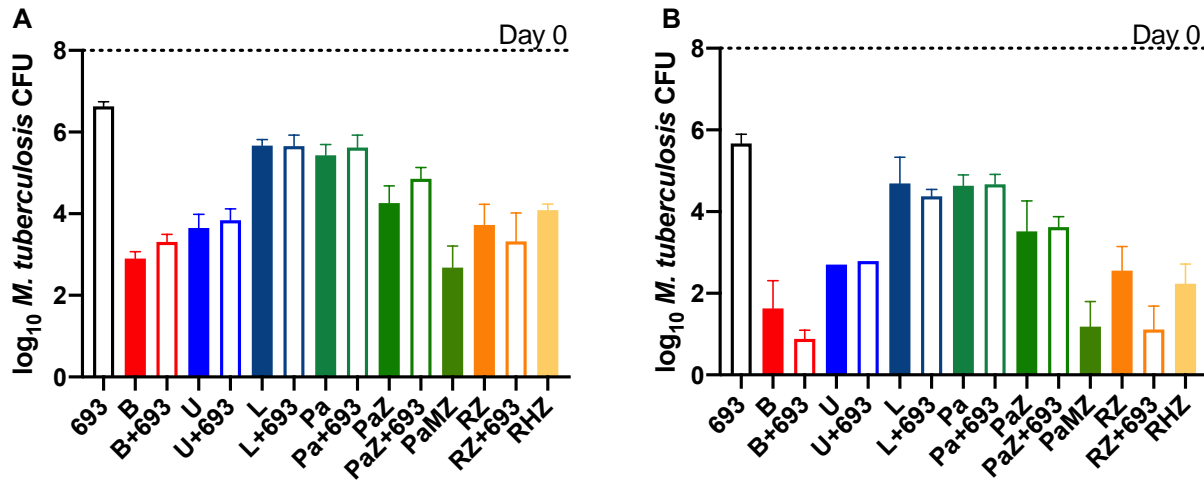
153 FIG 1. Dose-response relationship for **GSK138** in an acute mouse infection model of TB. Each  
154 point represents data from an individual mouse that received **GSK138** administered orally once  
155 daily for 8 days.

156

157 This acute infection model measures antitubercular activity on fast-growing bacteria  
158 (22). Treatment is administered for 8 consecutive days, starting 1 day after infection.  
159 Because the bacterial load reduction previously observed with **GSK693** was similar in  
160 both acute and chronic murine TB models (20), we performed a full dose-response  
161 study only in the acute model to characterize the compound and estimate the optimal  
162 dose for future combination studies. **GSK138** induced a net killing of the bacteria at the  
163 highest doses. The ED<sub>99</sub> (the dose producing a 2-log<sub>10</sub> reduction in colony-forming units  
164 [CFUs] compared to untreated control mice) for **GSK138** was 57 mg/Kg (95%  
165 confidence interval [CI]: 50-67 mg/Kg) and the dose of **GSK138** at which the 90% of the  
166 maximum bactericidal effect was achieved (ED<sub>max</sub>) was 167 mg/Kg (95%CI: 125->290  
167 mg/Kg). The whole blood area under the concentration-time curve over 24 hours post-  
168 dose (AUC<sub>0-24h</sub>) at steady-state associated with this ED<sub>max</sub> (AUC<sub>EDmax</sub>) was 68,544

169 ng\*h/mL. Comparison with previous data suggests that **GSK138** is as efficacious as  
170 **GSK693** at a lower exposure, and therefore **GSK138** has the potential for a lower dose  
171 prediction in humans.

172 Ultimately, any antitubercular drug must be used in combination with other anti-  
173 tubercular drugs to treat active TB. The success of any new regimen will depend on the  
174 properties of these drugs and how they work in combination. **GSK693** and **GSK138**  
175 showed suitable profiles to justify investigation of the efficacy of these DIs in  
176 combination with other drugs in animal models. Firstly, **GSK693** was selected as a tool  
177 compound to learn about the chemical series and its interactions with potential  
178 companion drugs. Experiment 1 was performed in a well-established high-dose aerosol  
179 infection model (23) with the following objectives: 1) to evaluate its ability to replace  
180 isoniazid (H) in combination with rifampicin (R) and pyrazinamide (Z) in the core first-  
181 line regimen, 2) to evaluate its ability to replace moxifloxacin (M) in combination with  
182 pretomanid (Pa) and pyrazinamide in the novel PaMZ regimen, and 3) to evaluate its  
183 contribution to the bactericidal activity of 2-drug combinations including bedaquiline (B),  
184 sutezolid (U), linezolid (L) and pretomanid (Figure 2).



185  
186 FIG 2. Mean ( $\pm$  SD) lung CFU counts at D0 and after 4 (A) or 8 (B) weeks of treatment in Expt  
187 1. In combination with RZ, but not with other drugs, **GSK693** showed significantly enhanced  
188 antibacterial activity at week 8 (B) but not at week 4 (A). Open bars show lung CFU counts with  
189 the addition of **GSK693** to drugs shown in solid bars. Drug doses: R = rifampicin 10 mg/Kg, Z =  
190 pyrazinamide 150 mg/Kg, H = isoniazid 10 mg/Kg, 693 = **GSK693** 300 mg/Kg, Pa = pretomanid  
191 50 mg/Kg, M = moxifloxacin 100 mg/Kg, B = bedaquiline 25 mg/Kg, L = linezolid 100 mg/Kg, U  
192 = sutezolid 50 mg/Kg.

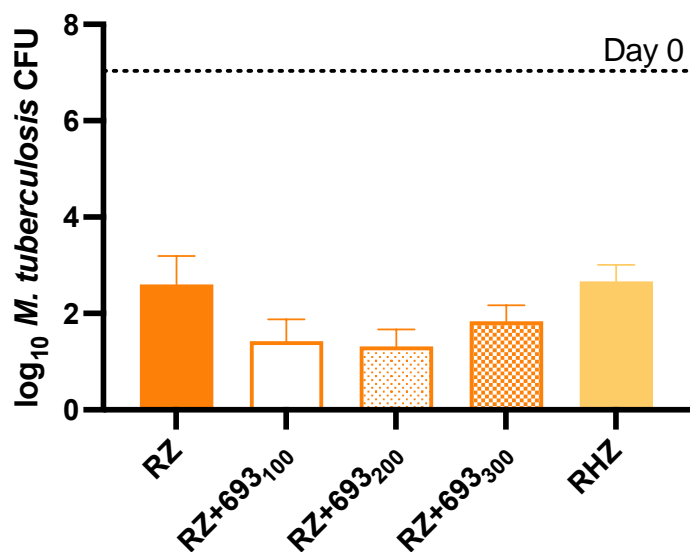
193 In this model, in which untreated mice routinely succumb to infection with lung CFU  
194 counts above 8  $\log_{10}$  within the first 3-4 weeks after infection, **GSK693** (300 mg/Kg)  
195 reduced the lung CFU counts by 1.34 and 2.33  $\log_{10}$  after 4 and 8 weeks of treatment,  
196 respectively. This bactericidal effect approached that of linezolid or pretomanid. No  
197 additive effect was observed when **GSK693** was combined with sutezolid, linezolid or  
198 pretomanid, nor was it as effective as moxifloxacin in combination with pretomanid and  
199 pyrazinamide. However, the combination of **GSK693** with rifampicin and pyrazinamide  
200 (RZ) was significantly more active than RZ alone or in combination with isoniazid after 8  
201 weeks of treatment ( $p < 0.05$ ). Notably, the combination of **GSK693** with bedaquiline also

202 resulted in greater activity after 8 weeks of treatment ( $p=0.08$ ) than that observed with  
203 bedaquiline alone. This additive effect of **GSK693** was attributable to its prevention of  
204 selection of bedaquiline-resistant mutants, as emergence of bedaquiline resistance was  
205 observed in 2 of the 4 mice treated with bedaquiline alone for 8 weeks, consistent with  
206 previous results (24). Excluding these 2 mice from the analysis revealed no difference  
207 between treatment with bedaquiline alone and bedaquiline plus **GSK693**.

208 The promising result observed with RZ+**GSK693** (in Exp. 1) prompted a follow-up  
209 experiment to confirm the additive effect of **GSK693**, evaluate the dose-response  
210 relationship for **GSK693** and explore potential drug-drug interactions in the RZ+**GSK693**  
211 combination.

212 As observed in Experiment 1, the addition of **GSK693**, but not isoniazid, significantly  
213 increased the activity of the RZ combination in Experiment 2 (Figure 3).

214



215  
216 FIG 3. Mean ( $\pm$  SD) lung CFU counts at D0 and after 8 weeks of treatment in Experiment 2.  
217 693 = **GSK693** significantly enhanced, in a non-dose-dependent manner, the activity of the RZ

218 (rifampicin, 10 mg/Kg, plus pyrazinamide 150 mg/Kg) combination. Isoniazid (10 mg/Kg) did not  
219 enhance the activity of the combination. **GSK693** dose (in mg/Kg) is indicated in subscripts.

220

221 The magnitude of the additive effect was also similar between experiments. The  
222 addition of **GSK693** at 300 mg/Kg to RZ reduced the lung CFU counts by an additional  
223 1.44 log in Experiment 1, as compared to a reduction of 0.76 log (p<0.05 vs RZ) in  
224 Experiment 2. Remarkably, however, greater reductions of 1.17 and 1.28 log (p<0.01  
225 and 0.001 vs RZ, respectively) were observed when **GSK693** was used at 100 and 200  
226 mg/Kg, respectively, in Experiment 2.

227 Although the sparse sampling prevented a formal assessment of the PK profile, the  
228 apparent lack of **GSK693** dose response was not explained by the **GSK693** exposures  
229 at the 100, 200 and 300 mg/Kg doses (Table 3).

230 TABLE 3. Data obtained from monocompartmental model of sparse plasma sampling  
231 concentrations in the combination study. A blood/plasma ratio of 1.79 was used to transform the  
232 plasma parameters to blood values.

<b>GSK693 Dose</b>	<b>Plasma AUC<sub>0-24h</sub> (ng·h/mL)</b>	<b>Blood AUC<sub>0-24h</sub> (ng·h/mL)</b>
<b>100 mg/Kg</b>	12,867	23,032
<b>200 mg/Kg</b>	27,337	48,933
<b>300 mg/Kg</b>	64,866	116,110

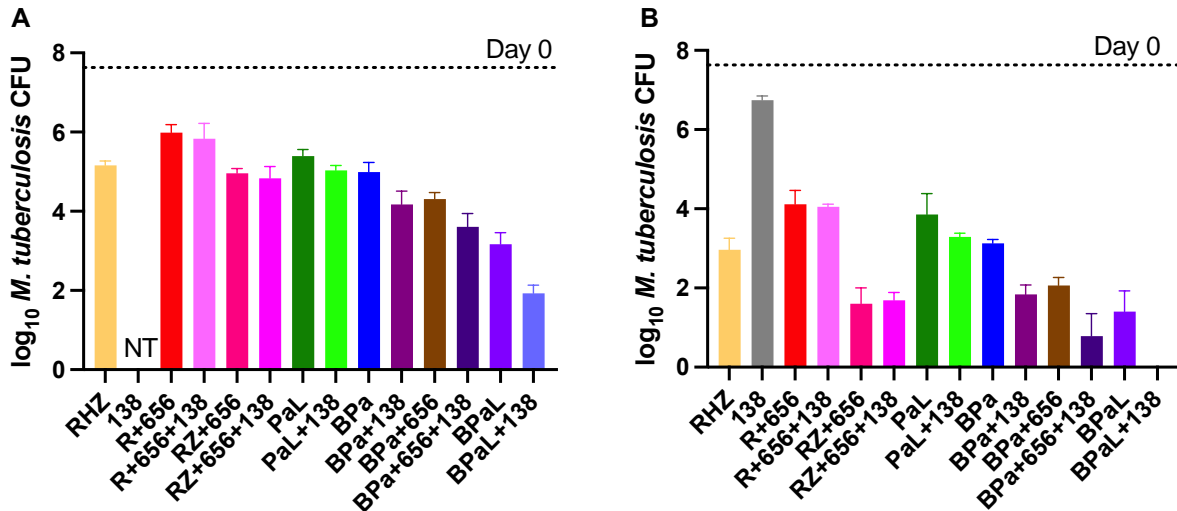
233

234 Interestingly, the observed effect of **GSK693** in combination was achieved at a lower  
235 exposure than that needed to achieve the maximum effect in monotherapy in the acute  
236 infection model (110,200 ng·h/mL). Based upon the potential for drug-drug interactions,

237 rifampicin was administered 1 hour prior to other drugs (25). Plasma exposure of  
238 rifampicin ( $AUC_{0-24h} = 68,544 \text{ ng}\cdot\text{h}/\text{mL}$ ) when co-administered with pyrazinamide  
239 showed no evidence of a higher exposure that could explain the increase in the efficacy  
240 of the combination when compared to prior data for rifampicin when co-administered  
241 with pyrazinamide ( $AUC_{0-24h} = 160,600 \text{ ng}\cdot\text{h}/\text{mL}$ ) (25) or as monotherapy at 10 mg/kg  
242 ( $AUC_{0-24h} = 87,200 \text{ to } 142,100 \text{ ng}\cdot\text{h}/\text{mL}$ ) (26).

243 The result from the combination of **GSK693** with RZ proved to be superior to the first-  
244 line treatment (RHZ). This result encouraged further combination experiments, now with  
245 **GSK138**.

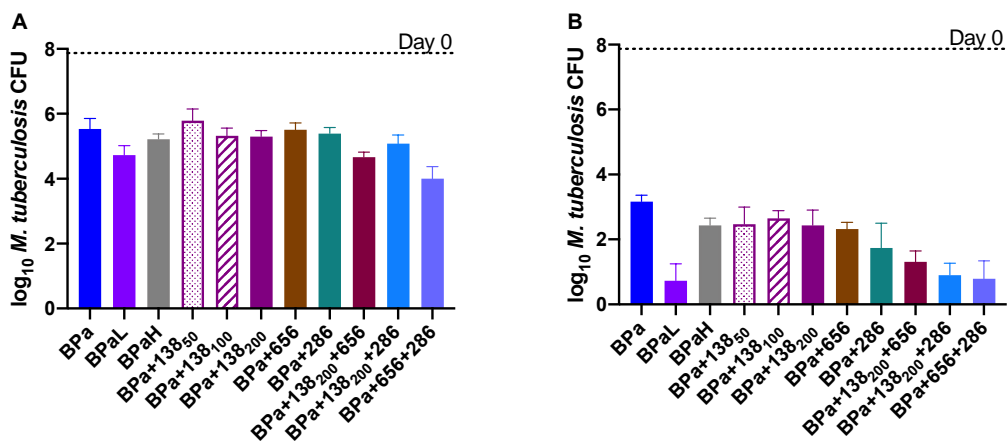
246 A major objective of Experiment 3 was to determine the effect of adding **GSK138** to the  
247 novel regimen of bedaquiline, pretomanid, and linezolid (BPaL) recently approved for  
248 treatment of XDR and treatment-intolerant or non-responsive MDR TB and the effect of  
249 substituting **GSK138** for either bedaquiline or linezolid. The experiment also included  
250 the novel LeuRS inhibitor GSK3036656 (GSK656) (27, 28) that is now in phase 2  
251 clinical trials. The objectives of this experiment were the following: 1) to evaluate the  
252 contribution of **GSK138** to the efficacy of 3- and 4-drug combinations based on the BPa  
253 backbone, and 2) to evaluate the effect of adding **GSK138** to the combination of  
254 rifampicin plus GSK656, with or without pyrazinamide (Figure 4).



255 FIG 4. The direct InhA inhibitor **GSK138** enhanced the activity of the BPa, BPaL and  
256 BPa+GSK656 combinations after 4 weeks (A) or 8 weeks (B) of treatment. After 8 weeks of  
257 treatment, the BPaL+**GSK138** regimen rendered mouse lungs culture negative. Data are  
258 presented as mean ( $\pm$  SD) lung CFU counts. R = rifampicin 10 mg/Kg, Z = pyrazinamide 150  
259 mg/Kg, H = isoniazid 10 mg/Kg, 138 = **GSK138** 200 mg/Kg, 656 = GSK656 (sulfate salt) 10  
260 mg/Kg, Pa = pretomanid 50 mg/Kg, B = bedaquiline 25 mg/Kg, L = linezolid 100 mg/Kg. NT =  
261 not tested.

262 The addition of **GSK138** to BPaL, its BPa backbone, or the novel BPa+GSK656  
263 regimen significantly increased the activity of each combination after 4 weeks ( $p<0.01$ )  
264 and after 8 weeks ( $p<0.0001$ ) of treatment. Indeed, the 4-drug combination of BPaL plus  
265 **GSK138** was the only regimen tested to render all mice culture-negative after 8 weeks  
266 of treatment. After 8 weeks of treatment, the activity of the 3- and 4-drug regimens  
267 containing BPa plus **GSK138**, with or without GSK656, were statistically  
268 indistinguishable from that of BPaL and significantly superior to the first-line RHZ  
269 regimen ( $p<0.0001$ ). The addition of **GSK138** did not significantly increase the activity of  
270 PaL, R+GSK656, or RZ+GSK656.

271 Experiment 4 (Figure 5) was performed to confirm the contribution of **GSK138** to the  
272 BPa backbone, this time including a range of **GSK138** doses. The experiment also  
273 included isoniazid as a comparator and combinations with GSK656 and the novel  
274 cholesterol-dependent inhibitor GSK2556286 (GSK286) (29) which is currently being  
275 investigated in a first time in human (FTIH) study to evaluate its safety, tolerability, and  
276 pharmacokinetics (NCT04472897).



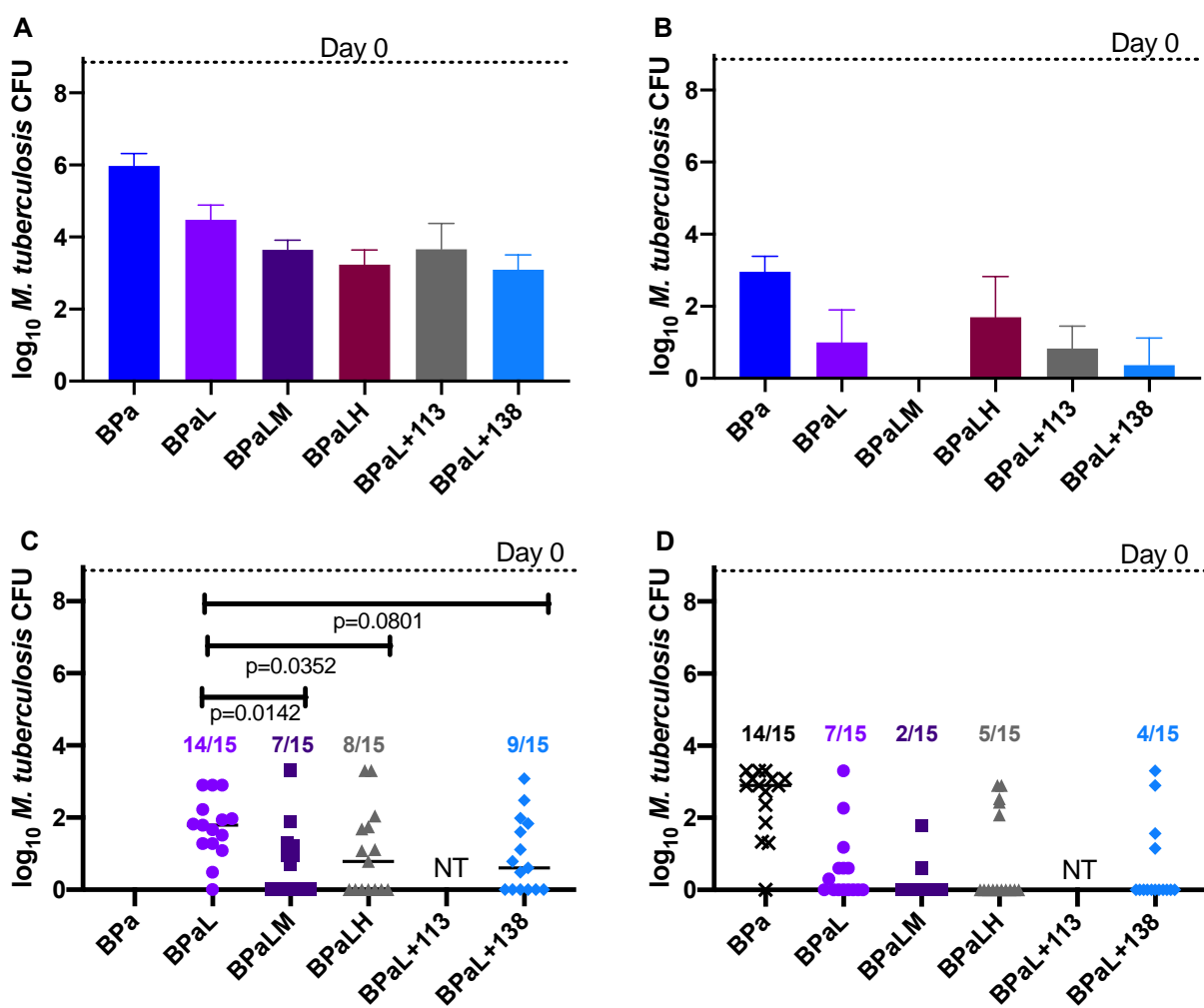
277

278 FIGURE 5. **GSK138** significantly enhanced the activity of BPa and BPa-based regimens at 4  
279 weeks (A) or 8 weeks (B), particularly in combination with GSK286. In combination with  
280 GSK656 or GSK286, the 200 mg/Kg dose of **GSK138** was used. Data are presented as mean  
281 ( $\pm$  SD) lung CFU counts B = bedaquiline, 25 mg/Kg; Pa = pretomanid, 100 mg/Kg, L = linezolid,  
282 100 mg/Kg, H = isoniazid 10 mg/Kg, 286 = GSK286, 50 mg/Kg, 656 = GSK656 (hydrochloride  
283 salt), 10 mg/Kg. **GSK138** dose (in mg/Kg) is indicated in subscripts.

284

285 The results reaffirmed the additive effects of **GSK138** when added to BPa for 8 weeks  
286 of treatment, and similar results were observed with the addition of isoniazid or GSK656  
287 to BPa. No dose-response of **GSK138** was evident after 8 weeks; and unlike in

288 Experiment 3, BPa plus **GSK138** was less effective than BPaL ( $p<0.01$  after 4 and 8  
289 weeks). However, as observed in Experiment 3, the additive 4-drug combination of  
290 BPa+GSK656 with **GSK138** was statistically indistinguishable from BPaL, as was the  
291 combination of BPa+GSK286 with **GSK138**. These 4-drug combinations of  
292 BPa+**GSK138** plus either GSK656 or GSK286 also had bactericidal activity similar to  
293 BPa+GSK656+GSK286 after 8 weeks of treatment.



294  
295 FIG 6. The addition of an InhA inhibitor or moxifloxacin enhanced the bactericidal and sterilizing  
296 activity of the BPaL regimen. After both 4 weeks (A) and 8 weeks (B), the addition of

297 moxifloxacin, isoniazid, NITD-113, or **GSK138** to BPaL enhanced the bactericidal activity  
298 compared to BPaL alone (with the exception of isoniazid at week 8). Data are presented as  
299 mean ( $\pm$  SD) lung CFU counts. The proportion of mice relapsing after 8 weeks of treatment,  
300 followed by 12 weeks of no treatment (C) was statistically significantly lower in the presence of  
301 either moxifloxacin or isoniazid and approached statistical significance with **GSK138**. There  
302 were fewer relapses after 12 weeks of treatment and 12 weeks of follow-up (D) with the addition  
303 of a fourth drug, although these differences were not statistically significant. The proportions of  
304 mice relapsing are indicated above the symbols for lung CFU counts. B = bedaquiline, 25  
305 mg/Kg, Pa = pretomanid, 100 mg/Kg, L = linezolid, 100 mg/Kg, M = moxifloxacin 100 mg/Kg, H  
306 = isoniazid 10 mg/Kg, NITD-113 = prodrug for NITD-916 (see Introduction) 150 mg/Kg, 138 =  
307 **GSK138** 200 mg/Kg. NT = not tested.

308

309 Given the superior bactericidal activity of the BPaL plus **GSK138** regimen compared to  
310 BPaL alone in Experiment 3, Experiment 5 was performed to determine whether  
311 addition of GSK138 to BPaL could shorten the duration of treatment needed to prevent  
312 relapse (Figure 6). Comparator regimens included BPaL plus one of the following:  
313 isoniazid, NITD-113 (prodrug for NITD-916, a previously reported DII based on a  
314 different scaffold than **GSK138**) (19) and moxifloxacin (M). As observed in Experiment  
315 3, the addition of **GSK138** at a dose of 200 mg/Kg significantly increased the  
316 bactericidal activity of BPaL after 4 weeks of treatment ( $p<0.01$ ), as did isoniazid  
317 ( $p<0.01$ ), while there was a trend towards enhanced activity with NITD-113 ( $p=0.11$ )  
318 and moxifloxacin ( $p=0.10$ ). BPaL+**GSK138** resulted in fewer culture-positive mice and a  
319 lower mean CFU count after 8 weeks compared to BPaL and BPaL plus other InhA  
320 inhibitors, although these differences were not statistically significant. Only the BPaLM

321 regimen rendered all mice culture-negative at this time point. Similarly, the addition of  
322 **GSK138**, isoniazid or moxifloxacin to BPaL each reduced the proportion of mice  
323 relapsing after 8 and 12 weeks of treatment compared to BPaL alone, although the  
324 differences were statistically significant only after 8 weeks of treatment with moxifloxacin  
325 or isoniazid, as shown in Figure 6C.

## 326 DISCUSSION

327 The thiadiazole-based DIs (namely **GSK693**) proved capable of replacing isoniazid in  
328 the first-line regimen. In fact, the bactericidal activity of the regimen increased with this  
329 substitution and **GSK693** increased the activity of the rifampicin-pyrazinamide  
330 combination. These results suggest that use of a DI instead of isoniazid could also  
331 increase the sterilizing activity of the regimen. The superior activity of the DI in this  
332 regimen may be the result of superior killing of phenotypically INH-tolerant persisters  
333 that have relatively lower *katG* expression, whether stochastically or in response to  
334 stress (30). Further development of thiadiazole DIs could yield superior first-line  
335 regimens containing rifamycins and pyrazinamide.

336 The thiadiazole-based DIs (namely **GSK138**) also proved capable of increasing the  
337 bactericidal and sterilizing activity of BPa-based regimens. BPaL is an effective 6-month  
338 all-oral regimen for XDR-TB and difficult-to-treat MDR-TB cases (31, 32). The improved  
339 efficacy observed with the addition of **GSK138** suggests that this or another DI could  
340 further improve the BPaL regimen by increasing the overall cure rate, shortening  
341 treatment duration and/or reducing the emergence of drug resistance. Considering the  
342 strong overall activity of BPa+**GSK693** and **GSK693**'s ability to prevent selection of  
343 bedaquiline-resistant mutants, the DIs of this class could also reduce the need for

344 linezolid, the most toxic component of the BPaL regimen allowing lower doses and/or  
345 shorter durations of linezolid.

346 The use of thiadiazole DIs alone or in combination with GSK656 to replace linezolid  
347 entirely, if proven safe, could enable the use of BPa-based regimens as alternative,  
348 more universally active, first-line regimens that would be less affected by isoniazid  
349 monoresistance or MDR.

350 Although not the focus of this report, we observed that the addition of moxifloxacin to  
351 BPaL improved the bactericidal and sterilizing activity of the regimen. BPaL and BPaLM  
352 were studied in the TB-PRACTECAL trial (ClinicalTrials.gov Identifier: NCT02589782).  
353 Our results, which were obtained before the start of the trial, predicted superior efficacy  
354 of the 4-drug combination. Indeed, a higher rate of sputum culture conversion at 8  
355 weeks was observed in TB-PRACTECAL participants receiving treatment with BPaLM  
356 vs. BPaL (77% vs. 46%) (33).

357 This research adds to the limited knowledge of the activity of direct InhA inhibitors in  
358 combination with new and existing TB drugs. The results suggest that a direct InhA  
359 inhibitor (e.g., **GSK138** and **GSK693**) could be a promising partner in novel drug  
360 regimens, enhancing their efficacy and/or preventing the selection of bedaquiline-  
361 resistant mutants. These findings increase our understanding of the mechanism of  
362 action of direct inhibitors of InhA and provide further impetus to continue exploiting InhA  
363 as a promising target for TB drug development.

364 **MATERIALS AND METHODS**

365 The human biological samples were sourced ethically, and their research use was in  
366 accord with the terms of the informed consents under an IRB/EC approved protocol. All

367 animal studies performed by GSK were ethically reviewed and carried out in  
368 accordance with European Directive 2010/63/EEC and the GSK Policy on the Care,  
369 Welfare and Treatment of Animals. All animal studies performed at Johns Hopkins  
370 University (JHU) were conducted in accordance with the GSK Policy on the Care,  
371 Welfare and Treatment of Laboratory Animals and were approved by the Institutional  
372 Animal Care and Use Committee of JHU.

373 **Chemistry.**

374 A micromilling method was applied to **GSK138** for particle size reduction in order to  
375 obtain a micronized GSK138 that was used in *in vivo* experiments. The Mixer Mill MM  
376 301 (Retsch) was used at a frequency of 20 Hz for four cycles of 5 minutes.

377 NMR spectra were recorded on an Agilent Inova 600 MHz spectrometer equipped with  
378 a 5 mm Triple Resonance Gradient Probe IDTG600-5 (experiments run under software  
379 version vnmr3.2 Revision A). Measurements were made at room temperature in DMSO-  
380 *d*6 solvent. The chemical shift (*d*) values are expressed in parts per million (ppm) and  
381 coupling constants are in Hertz (Hz). The chemical shifts ( $\delta$ ) were given relative to the  
382 residual  $^1\text{H}$  and  $^{13}\text{C}$  signals of the solvent peak as an internal standard: in  $^1\text{H}$  NMR (600  
383 MHz)  $\delta$  2.49 ppm (quin,  $\text{C}_2\text{D}_5\text{HOS}$ ) for DMSO-*d*<sub>6</sub>; in  $^{13}\text{C}$  NMR (150 MHz)  $\delta$  40.07 ppm  
384 (sept) for DMSO-*d*<sub>6</sub>. Legend: s = singlet, d = doublet, sept = septet, br = broad signal.

385 LC-MS purity data were collected using a Waters Acquity UPLC instrument coupled with  
386 Waters Acquity single quadrupole mass and photodiode array detectors. High-resolution  
387 MS (HRMS) was performed on a QSTAR Elite System mass spectrometer.  $^1\text{H}$  NMR  
388 (600 MHz, DMSO-*d*<sub>6</sub>):  $\delta$  10.67 (s, 1H, NH), 7.26 (s, 1H, OH), 7.18 (s, 1H), 7.09 (s, 1H),  
389 5.79 (s, 1H), 5.16 (s, 2H), 2.59 (s, 3H), 2.29 (s, 3H), 2.26 (s, 3H), 1.97 (s, 3H).  $^{13}\text{C}$  NMR

390 (150 MHz, DMSO-*d*<sub>6</sub>): δ 175.96, 166.46, 166.29, 164.69, 152.55, 152.26, 147.61,  
391 140.88, 116.47, 115.38, 94.56, 74.68, 48.82, 28.98, 19.29, 17.51, 11.53. HRMS (ESI)  
392 *m/z*: calcd for C<sub>17</sub>H<sub>19</sub>N<sub>7</sub>OS<sub>3</sub> [M + H]<sup>+</sup>, 434.0891; found, 434.0889.

393 **Permeability studies.** Studies were performed as described by Polli et al. (34), with  
394 minor modifications. GF120918 was used as the inhibitor of P-gp. Apical-to-basolateral  
395 (A-to-B) and basolateral-to-apical (B-to-A) transport were studied across MDR1-MDCKII  
396 cell monolayers in the absence and presence of the P-gp inhibitor GF120918, and the  
397 Papp (intrinsic apparent permeability) was estimated in both directions with or without  
398 inhibitor.

399 **Solubility studies.** Solubility assays were performed using a miniaturized shake flask  
400 method. 10 mM stock solutions of each test compound were used to prepare calibration  
401 standards (10-220 μM) in DMSO, and to spike (1:50) duplicate aqueous samples of  
402 FaSSIF (simulating fasting state biorelevant media, pH 6.5), with a final DMSO  
403 concentration of 2%. After shaking for 2 hours at 25 °C, the solutions were filtered and  
404 analysed by means of HPLC-DAD (Agilent 1200 Rapid Resolution HPLC with a diode  
405 array detector). Best fit calibration curves were constructed using the calibration  
406 standards, which were used to determine the aqueous samples solubility (35).

407 **Bacterial strains.** *M. tuberculosis* H37Rv was mouse-passaged, frozen in aliquots and  
408 sub-cultured in Middlebrook 7H9 broth with 10% oleic acid-albumin-dextrose-catalase  
409 (OADC) (Fisher, Pittsburgh, PA) and 0.05% Tween 80 prior to high-dose mouse aerosol  
410 infection. MDR and XDR *M. tuberculosis* clinical isolates representing different  
411 resistance phenotypes belong to the collection of strains of the Vall d'Hebron hospital of  
412 Barcelona.

413 *M. tuberculosis* H37Rv and H37Rv-Luc were routinely propagated at 37°C in  
414 Middlebrook 7H9 broth (Difco) supplemented with 10% Middlebrook albumin-dextrose-  
415 catalase (ADC)(Difco), 0.2% glycerol and 0.05% (vol/vol) tyloxapol or on Middlebrook  
416 7H10 agar plates (Difco) supplemented with 10% (vol/vol) OADC (Difco). Hygromycin B  
417 was added to the medium (50 µg/mL) to ensure plasmid maintenance when propagating  
418 the H37Rv-Luc strain. This strain constitutively expresses the luciferase *luc* gene from  
419 *Photinus pyralis* (GenBank Accession Number M15077) cloned in a mycobacterial  
420 shuttle plasmid derived from pACE-1 (36).

421 **Intracellular MIC assay.** Frozen stocks of macrophage THP-1 cells (ATCC TIB-202)  
422 were thawed in RPMI-1640 medium (Sigma) supplemented with 10% fetal bovine  
423 serum (FBS) (Gibco), 2 mM L-glutamine (Sigma) and 1 mM sodium pyruvate (Sigma).  
424 THP-1 cells were passaged only five times and maintained without antibiotics between  
425 2–10 × 10<sup>5</sup> cells/mL at 37 °C in a humidified, 5% CO<sub>2</sub> atmosphere. THP-1 cells (3 ×  
426 10<sup>8</sup>) were simultaneously differentiated with phorbol myristate acetate (PMA, 40 ng/mL,  
427 Sigma) and infected for 4 hours at a multiplicity of infection (MOI) of 1:1 with a single  
428 cell suspension of H37Rv-Luc. After incubation, infected cells were washed four times  
429 to remove extracellular bacilli and resuspended (2 × 10<sup>5</sup> cells/mL) in RPMI medium  
430 supplemented with 10% FBS (Hyclone), 2 mM L-glutamine and pyruvate and dispensed  
431 in white, flat bottom 384-well plates (Greiner) in a final volume of 50 µL (max. 0.5%  
432 DMSO). Plates were incubated for 5 days under 5% CO<sub>2</sub> atmosphere, 37 °C, 80%  
433 relative humidity before growth assessment. The Bright-Glo™ Luciferase Assay System  
434 (Promega, Madison, WI) was used as cell growth indicator for the H37Rv-Luc strain.  
435 Luminescence was measured in an Envision Multilabel Plate Reader (PerkinElmer)

436 using the opaque 384-plate Ultra Sensitive luminescence mode, with a measurement  
437 time of 50 ms. A 90% reduction in light production was considered growth inhibition and  
438 the IC<sub>90</sub> value was interpolated from the dose response curve.

439 **Extracellular MIC assays.** MICs against the H37Rv strain were determined by broth  
440 dilution assay in Middlebrook 7H9 medium supplemented with 10% ADC. After  
441 incubating at 37 °C for six days, 25 µL resazurin solution (one tablet in 30 mL sterile  
442 PBS) was added to each well. Following incubation at 37 °C for two additional days, the  
443 lowest concentration of drug that inhibited 90% of resazurin conversion compared to  
444 internal DMSO control wells with no drug added was used to define MIC values.

445 MICs against clinical isolates of *M. tuberculosis* were determined using the  
446 mycobacteria growth indicator tubes (MGIT) system. Approximately 1 mg wet weight  
447 from a Lowenstein-Jensen slant, with an estimated bacterial load of 10<sup>8</sup> CFU/mL, was  
448 inoculated into McCartney vials containing 1 mL of distilled water and 5 glass beads.  
449 The mixtures were homogenized by vortexing for 1-3 minutes. The opacity of the  
450 suspensions was adjusted by the addition of sterile distilled water to that of a 0.5  
451 McFarland turbidity standard. 100 µL were used to inoculate MGIT vials containing  
452 serial dilutions of the compounds. MIC values were defined using the BACTEC MGIT  
453 960 System (Becton Dickinson) and following the manufacturer's instructions.

454 **HepG2 cytotoxicity assay.** HepG2 cells were cultured using Eagle's minimum  
455 essential media (EMEM) supplemented with 10% heat-inactivated FBS, 1% Non-  
456 Essential Amino Acid (NEAA), and 1% penicillin/streptomycin. Prior to addition of the  
457 cell suspension, 250 nL of test compounds per well were predispensed in Tissue culture  
458 -treated black clear-bottomed 384-well plates (Greiner, cat. no. 781091) with an Echo

459 555 instrument. After that, 25  $\mu$ L of HepG2 (cat. no. ATCC HB-8065) cells (~3000  
460 cells/well) grown to confluence in EMEM supplemented with 10% heat-inactivated FBS,  
461 1% NEAA, and 1% penicillin/streptomycin were added to each well with the reagent  
462 dispenser. Plates were allowed to incubate at 37 °C with 20% O<sub>2</sub> and 5% CO<sub>2</sub> for 48  
463 hrs. After incubation, the plates were equilibrated to room temperature before ATP  
464 levels were measured with the CellTiter Glo kit (Promega) as the cell viability read-out.  
465 25  $\mu$ L of CellTiter Glo substrate dissolved in the buffer was added to each well. Plates  
466 were incubated at room temperature for 10 min for stabilization of luminescence signal  
467 and read on a View Lux luminometer with excitation and emission filters of 613 and 655  
468 nm, respectively. The Tox<sub>50</sub> value corresponds to the concentration of the compound  
469 necessary to inhibit 50% of cell growth.

470 **Cell Health Assay.** This is a 3-parameter automated imaging cell-based assay to  
471 measure the cytotoxic effect of compounds in human liver-derived HepG2 cells. Using  
472 fluorescent staining, the key parameters measured in this assay are nuclear size,  
473 mitochondrial membrane potential and plasma membrane permeability. HepG2 cells  
474 (ATCC HB-8065) were incubated with the test compounds in 384-well plates. After 48  
475 hours, the staining cocktail was added. Hoechst 33342 is used to stain nuclei and  
476 quantify changes in nuclear morphology. Tetramethylrhodamine, methyl ester (TMRM)  
477 is a cationic dye that accumulates in healthy mitochondria that maintain a mitochondrial  
478 membrane potential and leaks out of mitochondria when the mitochondrial membrane  
479 potential is dissipated. TOTO-3 iodide labels nuclei of permeabilized cells and is used to  
480 measure plasma membrane permeability. Following 45 min of incubation with these  
481 stains, the plates were sealed using a black seal for reading on an INCell Analyzer 2000

482 (GE Healthcare). Each parameter measurement produces the percentages of cells  
483 which are 'LIVE' or 'DEAD'. The IC<sub>50</sub> is defined as the compound concentration that  
484 inhibits 50% of cell growth.

485 **Ames Assay.** The Ames assay was carried out as previously described (37) using all  
486 strains.

487 **hERG Assay.** hERG activity was measured as previously described (38).

488 **Hepatic microsome stability.** Human and animal microsomes and compounds were  
489 preincubated at 37 °C prior to addition of NADPH to final protein concentration of 0.5  
490 mg/mL and final compound concentration of 0.5 µM. Quantitative analysis was  
491 performed using specific LC-MS/MS conditions. The half-life, elimination rate constant,  
492 and intrinsic clearance (mL/min/g tissue) were determined. The well-stirred model was  
493 used to translate to *in vivo* Cl values (mL/min/Kg).

494 ***In vivo* pharmacokinetics analysis.** Single-dose pharmacokinetics experiments were  
495 performed in female C57BL/6 mice, 21-29 g, obtained from Charles River Laboratories  
496 (Wilmington, MA) and housed in cages in groups of three animals with water and food  
497 *ad libitum*. Animals were maintained for one week before the experiment.

498 The compound was dissolved in 20% Encapsin (Sigma-Aldrich), 5% DMSO (Sigma  
499 Aldrich) in saline solution (Sigma Aldrich) for intravenous administration and in 1%  
500 methylcellulose (Sigma-Aldrich) in water for oral administration.

501 For PK analysis, 25 µL of tail blood were collected by microsampling at 0.08 h, 0.25 h,  
502 0.5 h, 1 h, 2 h, 4 h, 6 h, 8 h and 24 h for intravenous pharmacokinetics and 0.25 h, 0.5  
503 h, 1 h, 2 h, 4 h, 6 h, 8 h and 24 h for oral pharmacokinetics.

504 **Assessment of acute efficacy in murine TB models.** Specific pathogen-free, 8-10  
505 week-old (18-20 grams) female C57BL/6 mice were purchased from Harlan  
506 Laboratories and were allowed to acclimate for one week. The experimental design for  
507 the acute assay has been previously described (22). In brief, mice were intratracheally  
508 infected with 100,000 CFU/mouse of *M. tuberculosis* H37Rv. Compounds were  
509 administered daily for 8 consecutive days starting 24 hours after infection. Lungs were  
510 harvested on day 9. All lung lobes were aseptically removed, homogenized and frozen.  
511 Homogenates were thawed and plated on 7H11 medium supplemented with 10%  
512 OADC plus 0.4% activated charcoal to reduce the effects of compound carryover. CFU  
513 were counted after 18 days of incubation at 37 °C. Log<sub>10</sub> CFU vs. dose data were  
514 plotted. A sigmoidal dose-response curve was fitted and used to estimate ED<sub>99</sub> and  
515 ED<sub>max</sub>. Data were analyzed using GraphPad software (Prism). The ED<sub>99</sub> was defined as  
516 the dose in mg/Kg that reduced the number of CFUs in the lungs of treated mice by  
517 99% compared to untreated infected mice. The ED<sub>max</sub> is the dose in mg/g that resulted  
518 in 90% of predicted maximal effect.

519 **Modelling and simulations**

520 The calculated exposures at ED<sub>max</sub> for **GSK138** and **GSK693** were obtained using the  
521 IV mouse PKs profiles fitting to a bicompartimental model to obtain those parameters to  
522 simulate the oral whole blood exposures at ED<sub>max</sub>. Additionally, a monocompartmental  
523 model was used to fit the experimental oral pharmacokinetic studies in non-infected  
524 mouse together with measured plasma concentrations obtained from the sparse  
525 sampling in the Experiment 2 in infected mice. Parameters obtained from this fitting  
526 were used to simulate the profile after **GSK693** administration at 100, 200 and 300

527 mg/Kg in the combination study and to calculate the associated exposures (see Table  
528 3).

529 **Blood and Plasma pharmacokinetic sampling and analysis**

530 Sample collection from non-infected animals (PK studies): Blood samples (25 µL) were  
531 taken from the lateral tail vein using a micropipette and were mixed, vortexed with 25 µL  
532 of saponin 0.1% and frozen at -80 °C until analysis.

533 Sample collection from infected animals: Mouse tail vein blood was collected at the  
534 indicated time points. Briefly, an incision was made in the lateral tail vein. 20-50 µL of  
535 blood was collected in BD Vacutainer® PST™ lithium heparin tubes from each mouse.  
536 The tubes were kept on ice before being centrifuged at 8000 rpm for 5 minutes. The  
537 supernatant plasma (15-30 µL) was transferred to labeled microcentrifuge tubes, frozen  
538 and stored at -80 °C and then shipped on dry ice to GSK for further analysis.

539 Sample pretreatment and LC-MS/MS analysis: 10 µL of plasma or blood samples  
540 thawed at ambient temperature was mixed with 200 µL of ACN:MeOH (80:20). After this  
541 protein precipitation step, samples were filtered using a 0.45 µm filter plate (Multiscreen  
542 Solvinert 0.45um FTPE, Millipore) and then filtered using a 0.2 µm filter (AcroPrep  
543 Advance 96 Filter Plate 350 µL, 0.2 µm PTFE) to ensure sterilization prior to LC-MS  
544 analysis.

545 An Acquity Ultra-Performance liquid chromatography (UPLC) system (Waters Corp.,  
546 Milford, MA, USA) coupled to a triple quadrupole mass spectrometer (API 4000™, AB  
547 Sciex, Foster City, CA, USA) was used for the analysis.

548 The chromatographic separation was conducted at 0.4 mL/min in an Acquity UPLC™  
549 BEH C18 column (50×2.1 mm i.d., 1.7 mm; Waters Corp.) at 40°C with acetonitrile  
550 (ACN) (SigmaAldrich) and 0.1% formic acid as eluents.

551 Sciex Analyst software was used for the data analysis. The non-compartmental data  
552 analysis (NCA) was performed with Phoenix WinNonlin software in order to determine  
553 pharmacokinetic parameters and exposure.

554 **High-dose aerosol mouse infection model.** Female specific pathogen-free BALB/c  
555 mice, aged 5-6 weeks, were purchased from Charles River (Wilmington, MA). Mice  
556 were infected by aerosol using the Inhalation Exposure System (Glas-col, Terre Haute,  
557 IN) using a log phase culture of *M. tuberculosis* H37Rv with an OD<sub>600</sub> of 0.8-1 to implant  
558 approximately 3.5-4 log<sub>10</sub> CFU in the lungs. Treatment started 2 weeks later (D0). Mice  
559 were sacrificed for lung CFU counts the day after infection and on D0 to determine the  
560 number of CFU implanted and the number present at the start of treatment,  
561 respectively.

562 **Antibiotic treatment.** Mice were treated with the drugs and drug combinations  
563 indicated in Figures 2 through 6 at the following doses (in mg/Kg body weight):  
564 bedaquiline (25), pretomanid (50 or 100), moxifloxacin (100), linezolid (100), isoniazid  
565 (10), rifampicin (10), sutezolid (50), **GSK138** (50, 100, or 200), **GSK693** (100, 200, or  
566 300), GSK656 (10), GSK286 (50), NITD-113 (150), and pyrazinamide (150). **GSK693**,  
567 **GSK138**, and GSK286 were formulated in 1% methylcellulose solution. GSK656 was  
568 formulated in distilled water. Other drugs were formulated as previously described (39-  
569 41). Bedaquiline and pretomanid were administered in back-to-back gavages and

570 separated from companion drugs by at least 3 hours. Rifampicin was administered  
571 alone at least one hour before any companion drug.

572 **Evaluation of drug efficacy.** Efficacy determinations were based on lung CFU counts  
573 after 4 or 8 weeks of treatment and, in one experiment, cohorts of mice were also kept  
574 for 12 weeks after completing 8 or 12 weeks of treatment to assess for relapse-free  
575 cure. At each time point, lungs were removed aseptically and homogenized in 2.5 mL of  
576 PBS. Serial 10-fold dilutions of lung homogenate were plated on selective 7H11 agar  
577 plates. To assess for relapse-free cure, the entire lung homogenate was plated. In  
578 experiments with bedaquiline, lung homogenates were plated on 7H11 agar  
579 supplemented with 0.4% activated charcoal to reduce drug carryover and doubling the  
580 concentrations of selective antibiotics in the media to mitigate binding to charcoal.

581 **Statistical analysis.** Group means were compared by one-way ANOVA with Dunnett's  
582 correction for multiple comparisons or by Student's t-test, as appropriate, using  
583 GraphPad Prism version 8.

584 **ACKNOWLEDGEMENTS**

585 We acknowledge funding by the European Union Seventh Framework Programme  
586 (FP7/2007- 2013) under grant agreement Nº 261378. We acknowledge Kala Barnes-  
587 Boyle for her technical assistance, Eva María López-Román and María José Rebollo-  
588 López for the MIC determination against mycobacteria and clinical isolates respectively,  
589 Raquel Gabarró, Jesús Gómez, Douglas J. Minick for conducting structural  
590 characterization experiments, Pablo Castañeda-Casado for the safety assessment and  
591 Fatima Ortega-Muro for her contribution in the review of the ADME and  
592 pharmacokinetics.

593 **REFERENCES**

- 594 1. World Health Organization. 2023. Global Tuberculosis Report 2023. Geneva
- 595 2. **Pai M, Kasaeva T, Swaminathan S.** 2022. Covid-19's Devastating Effect on
- 596 Tuberculosis Care - A Path to Recovery. *N Engl J Med* **386**:1490-1493.
- 597 3. **Bernstein J, Lott WA, Steinberg BA, Yale HL.** 1952. Chemotherapy of experimental
- 598 tuberculosis. V. Isonicotinic acid hydrazide (hydrazide) and related compounds. *Am Rev*
- 599 *Tuberc* **65**:357-364.
- 600 4. **Zhang Y, Heym B, Allen B, Young D, Cole S.** 1992. The catalase-peroxidase gene and
- 601 isoniazid resistance of *Mycobacterium tuberculosis*. *Nature* **358**:591-593.
- 602 5. **Quémard A, Sacchettini JC, Dessen A, Vilchez C, Bittman R, Jacobs WR, Jr.,**
- 603 **Blanchard JS.** 1995. Enzymatic characterization of the target for isoniazid in
- 604 *Mycobacterium tuberculosis*. *Biochemistry* **34**:8235-8241.
- 605 6. **Rozwarski DA, Grant GA, Barton DH, Jacobs WR, Jr., Sacchettini JC.** 1998.
- 606 Modification of the NADH of the isoniazid target (InhA) from *Mycobacterium*
- 607 *tuberculosis*. *Science* **279**:98-102.
- 608 7. **Vilchèze C, Wang F, Arai M, Hazbón MH, Colangeli R, Kremer L, Weisbrod TR,**
- 609 **Alland D, Sacchettini JC, Jacobs WR, Jr.** 2006. Transfer of a point mutation in
- 610 *Mycobacterium tuberculosis inhA* resolves the target of isoniazid. *Nat Med* **12**:1027-
- 611 1029.
- 612 8. **Dean AS, Zignol M, Cabibbe AM, Falzon D, Glaziou P, Cirillo DM, Köser CU,**
- 613 **Gonzalez-Angulo LY, Tosas-Auguet O, Ismail N, Tahseen S, Ama MCG, Skrahina A,**
- 614 **Alikhanova N, Kamal SMM, Floyd K.** 2020. Prevalence and genetic profiles of
- 615 isoniazid resistance in tuberculosis patients: A multicountry analysis of cross-sectional
- 616 data. *PLoS Med* **17**:e1003008.
- 617 9. **Fregonese F, Ahuja SD, Akkerman OW, Arakaki-Sanchez D, Ayakaka I, Baghaei P,**
- 618 **Bang D, Bastos M, Benedetti A, Bonnet M, Cattamanchi A, Cegielski P, Chien JY,**
- 619 **Cox H, Dedicoat M, Erkens C, Escalante P, Falzon D, Garcia-Prats AJ, Gegia M,**
- 620 **Gillespie SH, Glynn JR, Goldberg S, Griffith D, Jacobson KR, Johnston JC, Jones-**
- 621 **López EC, Khan A, Koh WJ, Kritski A, Lan ZY, Lee JH, Li PZ, Maciel EL, Galliez**
- 622 **RM, Merle CSC, Munang M, Narendran G, Nguyen VN, Nunn A, Ohkado A, Park**
- 623 **JS, Phillips PPJ, Ponnuraja C, Reves R, Romanowski K, Seung K, Schaaf HS,**
- 624 **Skrahina A, Soolingen DV, et al.** 2018. Comparison of different treatments for
- 625 isoniazid-resistant tuberculosis: an individual patient data meta-analysis. *Lancet Respir*
- 626 *Med* **6**:265-275.
- 627 10. **Gegia M, Winters N, Benedetti A, van Soolingen D, Menzies D.** 2017. Treatment of
- 628 isoniazid-resistant tuberculosis with first-line drugs: a systematic review and meta-
- 629 analysis. *Lancet Infect Dis* **17**:223-234.
- 630 11. **Stagg HR, Harris RJ, Hatherell HA, Obach D, Zhao H, Tsuchiya N, Kranzer K,**
- 631 **Nikolayevskyy V, Kim J, Lipman MC, Abubakar I.** 2016. What are the most
- 632 efficacious treatment regimens for isoniazid-resistant tuberculosis? A systematic review
- 633 and network meta-analysis. *Thorax* **71**:940-949.
- 634 12. **Stagg HR, Lipman MC, McHugh TD, Jenkins HE.** 2017. Isoniazid-resistant
- 635 tuberculosis: a cause for concern? *Int J Tuberc Lung Dis* **21**:129-139.
- 636 13. **Sulis G, Pai M.** 2020. Isoniazid-resistant tuberculosis: A problem we can no longer
- 637 ignore. *PLoS Med* **17**:e1003023.

638 14. **World Health Organization.** 2018. WHO treatment guidelines for isoniazid- resistant  
639 tuberculosis. Supplement to the WHO treatment guidelines for drug-resistant  
640 tuberculosis. Geneva.

641 15. **Brossier F, Boudinet M, Jarlier V, Petrella S, Sougakoff W.** 2016. Comparative study  
642 of enzymatic activities of new KatG mutants from low- and high-level isoniazid-resistant  
643 clinical isolates of *Mycobacterium tuberculosis*. *Tuberculosis (Edinb)* **100**:15-24.

644 16. **Dooley KE, Miyahara S, von Groote-Bidlingmaier F, Sun X, Hafner R, Rosenkranz  
645 SL, Ignatius EH, Nuermberger EL, Moran L, Donahue K, Swindells S, Vanker N,  
646 Diacon AH.** 2020. Early Bactericidal Activity of Different Isoniazid Doses for Drug  
647 Resistant TB (INHindsight): A Randomized Open-label Clinical Trial. *Am J Respir Crit  
648 Care Med* **201**:1416-1424.

649 17. **Seifert M, Catanzaro D, Catanzaro A, Rodwell TC.** 2015. Genetic mutations  
650 associated with isoniazid resistance in *Mycobacterium tuberculosis*: a systematic review.  
651 *PLoS One* **10**:e0119628.

652 18. **Rožman K, Sosič I, Fernandez R, Young RJ, Mendoza A, Gobec S, Encinas L.** 2017.  
653 A new 'golden age' for the antitubercular target InhA. *Drug Discov Today* **22**:492-502.

654 19. **Manjunatha UH, SP SR, Kondreddi RR, Noble CG, Camacho LR, Tan BH, Ng SH,  
655 Ng PS, Ma NL, Lakshminarayana SB, Herve M, Barnes SW, Yu W, Kuhen K,  
656 Blasco F, Beer D, Walker JR, Tonge PJ, Glynne R, Smith PW, Diagana TT.** 2015.  
657 Direct inhibitors of InhA are active against *Mycobacterium tuberculosis*. *Sci Transl Med*  
658 **7**:269ra263.

659 20. **Martínez-Hoyos M, Perez-Herran E, Gulten G, Encinas L, Álvarez-Gómez D,  
660 Alvarez E, Ferrer-Bazaga S, García-Pérez A, Ortega F, Angulo-Barturen I, Rullas-  
661 Trincado J, Blanco Ruano D, Torres P, Castañeda P, Huss S, Fernández Menéndez  
662 R, González Del Valle S, Ballell L, Barros D, Modha S, Dhar N, Signorino-Gelo F,  
663 McKinney JD, García-Bustos JF, Lavandera JL, Sacchettini JC, Jimenez MS,  
664 Martín-Casabona N, Castro-Pichel J, Mendoza-Losana A.** 2016. Antitubercular drugs  
665 for an old target: GSK693 as a promising InhA direct inhibitor. *EBioMedicine* **8**:291-  
666 301.

667 21. **Xia Y, Zhou Y, Carter DS, McNeil MB, Choi W, Halladay J, Berry PW, Mao W,  
668 Hernandez V, O'Malley T, Korkegian A, Sunde B, Flint L, Woolhiser LK,  
669 Scherman MS, Gruppo V, Hastings C, Robertson GT, Ioerger TR, Sacchettini J,  
670 Tonge PJ, Lenaerts AJ, Parish T, Alley M.** 2018. Discovery of a cofactor-independent  
671 inhibitor of *Mycobacterium tuberculosis* InhA. *Life Sci Alliance* **1**:e201800025.

672 22. **Rullas J, García JI, Beltrán M, Cardona PJ, Cáceres N, García-Bustos JF, Angulo-  
673 Barturen I.** 2010. Fast standardized therapeutic-efficacy assay for drug discovery against  
674 tuberculosis. *Antimicrob Agents Chemother* **54**:2262-2264.

675 23. **Nuermberger EL.** 2017. Preclinical Efficacy Testing of New Drug Candidates.  
676 *Microbiol Spectr* **5**.

677 24. **Almeida D, Ioerger T, Tyagi S, Li SY, Mdluli K, Andries K, Grosset J, Sacchettini J,  
678 Nuermberger E.** 2016. Mutations in pepQ Confer Low-Level Resistance to Bedaquiline  
679 and Clofazimine in *Mycobacterium tuberculosis*. *Antimicrob Agents Chemother*  
680 **60**:4590-4599.

681 25. **Grosset J, Truffot-Pernot C, Lacroix C, Ji B.** 1992. Antagonism between isoniazid and  
682 the combination pyrazinamide-rifampin against tuberculosis infection in mice.  
683 *Antimicrob Agents Chemother* **36**:548-551.

684 26. **Rosenthal IM, Williams K, Tyagi S, Peloquin CA, Vernon AA, Bishai WR, Grosset**  
685 **JH, Nuermberger EL.** 2006. Potent twice-weekly rifapentine-containing regimens in  
686 murine tuberculosis. *Am J Respir Crit Care Med* **174**:94-101.

687 27. **Li X, Hernandez V, Rock FL, Choi W, Mak YSL, Mohan M, Mao W, Zhou Y,**  
688 **Easom EE, Plattner JJ, Zou W, Pérez-Herrán E, Giordano I, Mendoza-Losana A,**  
689 **Alemparte C, Rullas J, Angulo-Barturen I, Crouch S, Ortega F, Barros D, Alley**  
690 **MRK.** 2017. Discovery of a Potent and Specific *M. tuberculosis* Leucyl-tRNA  
691 Synthetase Inhibitor: (S)-3-(Aminomethyl)-4-chloro-7-(2-  
692 hydroxyethoxy)benzo[c][1,2]oxaborol-1(3H)-ol (GSK656). *J Med Chem* **60**:8011-8026.

693 28. **Tenero D, Derimanov G, Carlton A, Tonkyn J, Davies M, Cozens S, Gresham S,**  
694 **Gaudion A, Puri A, Muliaditan M, Rullas-Trincado J, Mendoza-Losana A,**  
695 **Skingsley A, Barros-Aguirre D.** 2019. First-Time-in-Human Study and Prediction of  
696 Early Bactericidal Activity for GSK3036656, a Potent Leucyl-tRNA Synthetase Inhibitor  
697 for Tuberculosis Treatment. *Antimicrob Agents Chemother* **63**.

698 29. **Nuermberger EL, Martínez-Martínez MS, Sanz O, Urones B, Esquivias J, Soni H,**  
699 **Tasneen R, Tyagi S, Li SY, Converse PJ, Boshoff HI, Robertson GT, Besra GS,**  
700 **Abrahams KA, Upton AM, Mdluli K, Boyle GW, Turner S, Fotouhi N, Cammack**  
701 **NC, Siles JM, Alonso M, Escribano J, Lelievre J, Rullas-Trincado J, Pérez-Herrán**  
702 **E, Bates RH, Maher-Edwards G, Barros D, Ballell L, Jiménez E.** 2022. GSK2556286  
703 Is a Novel Antitubercular Drug Candidate Effective In Vivo with the Potential To  
704 Shorten Tuberculosis Treatment. *Antimicrob Agents Chemother* **66**:e0013222.

705 30. **Wakamoto Y, Dhar N, Chait R, Schneider K, Signorino-Gelo F, Leibler S,**  
706 **McKinney JD.** 2013. Dynamic persistence of antibiotic-stressed mycobacteria. *Science*  
707 **339**:91-95.

708 31. **Conradie F, Bagdasaryan TR, Borisov S, Howell P, Mikiashvili L, Ngubane N,**  
709 **Samoilova A, Skornykova S, Tudor E, Variava E, Yablonskiy P, Everitt D, Wills**  
710 **GH, Sun E, Olugbosi M, Egizi E, Li M, Holsta A, Timm J, Bateson A, Crook AM,**  
711 **Fabiane SM, Hunt R, McHugh TD, Tweed CD, Foraida S, Mendel CM, Spigelman**  
712 **M.** 2022. Bedaquiline-Pretomanid-Linezolid Regimens for Drug-Resistant Tuberculosis.  
713 *N Engl J Med* **387**:810-823.

714 32. **Conradie F, Diacon AH, Ngubane N, Howell P, Everitt D, Crook AM, Mendel CM,**  
715 **Egizi E, Moreira J, Timm J, McHugh TD, Wills GH, Bateson A, Hunt R, Van**  
716 **Niekerk C, Li M, Olugbosi M, Spigelman M.** 2020. Treatment of Highly Drug-  
717 Resistant Pulmonary Tuberculosis. *N Engl J Med* **382**:893-902.

718 33. **Nyang'wa BT.** 2021. SP-34 TB-PRACTECAL Stage 2 Trial Efficacy Results, abstr 52nd  
719 World Conference on Lung Health of the International Union Against Tuberculosis and  
720 Lung Disease (The Union), Paris, 22 October, 2021.

721 34. **Polli JW, Wring SA, Humphreys JE, Huang L, Morgan JB, Webster LO, Serabjit-**  
722 **Singh CS.** 2001. Rational use of in vitro P-glycoprotein assays in drug discovery. *J*  
723 *Pharmacol Exp Ther* **299**:620-628.

724 35. **Hill AP, Young RJ.** 2010. Getting physical in drug discovery: a contemporary  
725 perspective on solubility and hydrophobicity. *Drug Discov Today* **15**:648-655.

726 36. **Sorrentino F, Gonzalez del Rio R, Zheng X, Presa Matilla J, Torres Gomez P,**  
727 **Martinez Hoyos M, Perez Herran ME, Mendoza Losana A, Av-Gay Y.** 2016.  
728 Development of an Intracellular Screen for New Compounds Able To Inhibit

729                   *Mycobacterium tuberculosis* Growth in Human Macrophages. *Antimicrob Agents*  
730                   *Chemother* **60**:640-645.

731           37. **Maron DM, Ames BN.** 1983. Revised methods for the *Salmonella* mutagenicity test.  
732                   *Mutat Res* **113**:173-215.

733           38. **Gillie DJ, Novick SJ, Donovan BT, Payne LA, Townsend C.** 2013. Development of a  
734                   high-throughput electrophysiological assay for the human ether-à-go-go related  
735                   potassium channel hERG. *J Pharmacol Toxicol Methods* **67**:33-44.

736           39. **Lounis N, Veziris N, Chauffour A, Truffot-Pernot C, Andries K, Jarlier V.** 2006.  
737                   Combinations of R207910 with drugs used to treat multidrug-resistant tuberculosis have  
738                   the potential to shorten treatment duration. *Antimicrob Agents Chemother* **50**:3543-3547.

739           40. **Tyagi S, Nuernberger E, Yoshimatsu T, Williams K, Rosenthal I, Lounis N, Bishai  
740                   W, Grosset J.** 2005. Bactericidal activity of the nitroimidazopyran PA-824 in a murine  
741                   model of tuberculosis. *Antimicrob Agents Chemother* **49**:2289-2293.

742           41. **Williams KN, Stover CK, Zhu T, Tasneen R, Tyagi S, Grosset JH, Nuernberger E.**  
743                   2009. Promising antituberculosis activity of the oxazolidinone PNU-100480 relative to  
744                   that of linezolid in a murine model. *Antimicrob Agents Chemother* **53**:1314-1319.

745

746

747

